

Formation and Function of the Manganese(IV)/Iron(III) Cofactor in *Chlamydia trachomatis* Ribonucleotide Reductase[†]Wei Jiang,^{*,‡,§} Danny Yun,^{‡,||} Lana Saleh,^{‡,⊥} J. Martin Bollinger, Jr.,^{*,‡,§} and Carsten Krebs^{*,‡,§}

Department of Biochemistry and Molecular Biology and Department of Chemistry, The Pennsylvania State University, University Park, Pennsylvania 16802

Received September 15, 2008; Revised Manuscript Received November 12, 2008

ABSTRACT: The β_2 subunit of a class Ia or Ib ribonucleotide reductase (RNR) is activated when its carboxylate-bridged $\text{Fe}_2^{\text{II/III}}$ cluster reacts with O_2 to oxidize a nearby tyrosine (Y) residue to a stable radical (Y^\bullet). During turnover, the Y^\bullet in β_2 is thought to reversibly oxidize a cysteine (C) in the α_2 subunit to a thiyl radical (C^\bullet) by a long-distance (~ 35 Å) proton-coupled electron-transfer (PCET) step. The C^\bullet in α_2 then initiates reduction of the 2' position of the ribonucleoside 5'-diphosphate substrate by abstracting the hydrogen atom from C3'. The class I RNR from *Chlamydia trachomatis* (*Ct*) is the prototype of a newly recognized subclass (Ic), which is characterized by the presence of a phenylalanine (F) residue at the site of β_2 where the essential radical-harboring Y is normally found. We recently demonstrated that *Ct* RNR employs a heterobinuclear $\text{Mn}^{\text{IV}}/\text{Fe}^{\text{III}}$ cluster for radical initiation. In essence, the Mn^{IV} ion of the cluster functionally replaces the Y^\bullet of the conventional class I RNR. The *Ct* β_2 protein also autoactivates by reaction of its reduced ($\text{Mn}^{\text{II}}/\text{Fe}^{\text{II}}$) metal cluster with O_2 . In this reaction, an unprecedented $\text{Mn}^{\text{IV}}/\text{Fe}^{\text{IV}}$ intermediate accumulates almost stoichiometrically and decays by one-electron reduction of the Fe^{IV} site. This reduction is mediated by the near-surface residue, Y222, a residue with no functional counterpart in the well-studied conventional class I RNRs. In this review, we recount the discovery of the novel Mn/Fe redox cofactor in *Ct* RNR and summarize our current understanding of how it assembles and initiates nucleotide reduction.

Ribonucleotide reductases (RNRs)¹ catalyze the reduction of ribonucleotides to deoxyribonucleotides, the building blocks for DNA. They provide the only de novo pathway for deoxyribonucleotide synthesis and are thus essential to all known life. Their central role in nucleotide metabolism

makes them important targets for anticancer and antiviral therapeutics (1). It is thought that the evolution of the first RNR initiated the transition from the use of RNA as the primary information-encoding molecule (in the "RNA world") to the use of DNA (in the "DNA world") (2, 3).

The RNR reaction involves replacement by hydrogen of the hydroxyl group on the 2'-carbon of the nucleoside di- or triphosphate (NDP or NTP) substrate. This chemically difficult replacement occurs by a free-radical mechanism (4). Evidence suggests that all known RNRs share a common fundamental strategy for catalysis, in which a transient cysteine thiyl radical (C^\bullet) in the active site (5–8) initiates the reduction by abstracting the 3'-hydrogen atom (9). Following replacement of the 2'-hydroxyl group with a hydrogen, the H^\bullet is returned to C3', regenerating the C^\bullet .

Although all RNRs apparently use this catalytic strategy, none possesses a C^\bullet in its resting state. Rather, the 3'-H-abstracting radical is produced at the beginning of each turnover and reduced back to the resting cysteine at the end (10–12). RNRs from different organisms have been divided into three classes primarily on the basis of the cofactor and mechanism that each employs for reversible C^\bullet production (2, 4). The enzymes from aerobically growing *Escherichia coli* (*Ec*), most eukaryotes (including all mammals), and herpes simplex I virus belong to class I. The C^\bullet -

[†] This work was supported by the National Institutes of Health (Grant GM-55365 to J.M.B. and C.K.), the Beckman Foundation (Young Investigator Award to C.K.), and the Dreyfus Foundation (Teacher Scholar Award to C.K.).

* To whom correspondence should be addressed. W.J.: Department of Chemistry, 318 Chemistry Building, University Park, PA 16802; phone, (814) 863-5685; fax, (814) 865-2927; e-mail, wuj101@psu.edu. J.M.B.: Department of Chemistry, 336 Chemistry Building, University Park, PA 16802; phone, (814) 863-5707; fax, (814) 865-2927; e-mail, jmb21@psu.edu. C.K.: Department of Chemistry, 332 Chemistry Building, University Park, PA 16802; phone, (814) 865-6089; fax, (814) 865-2927; e-mail, ckrebs@psu.edu.

[‡] Department of Biochemistry and Molecular Biology.

[§] Department of Chemistry.

^{||} Present address: Department of Chemistry, Massachusetts Institute of Technology, Cambridge, MA 02139.

[⊥] Present address: New England Biolabs, 240 County Rd., Ipswich, MA 01938.

¹ Abbreviations: C^\bullet , cysteinyl radical; CDP, cytidine 5'-diphosphate; *Ct*, *Chlamydia trachomatis*; dCDP, 2'-deoxycytidine 5'-diphosphate; *Ec*, *Escherichia coli*; EPR, electron paramagnetic resonance; NH_2Y , 3-aminotyrosine; $\text{N}_3\text{-ADP}$, 2'-azido-2'-deoxyadenosine 5'-diphosphate; NDP, nucleoside 5'-diphosphate; dNDP, 2'-deoxynucleoside 5'-diphosphate; NTP, nucleoside 5'-triphosphate; PCET, proton-coupled electron transfer; RNR, ribonucleotide reductase; Y^\bullet , tyrosyl radical.

generating cofactor in each of these RNRs is a stable tyrosyl radical (Y[•]) in the proximity of a (μ -oxo)-Fe₂^{III/III} cluster (12, 13). The cofactor is found in the enzyme's homodimeric β_2 subunit. It is generated when the Fe₂^{III/II} form of the cluster reacts with O₂ to oxidize the Y residue by one electron to the Y[•] (13) (vide infra). The active holoenzyme is a dissociable 1:1 complex² of the homodimeric β_2 subunit and the homodimeric catalytic subunit, α_2 , which contains the active site for substrate reduction and the binding sites for allosteric effectors (2). To initiate turnover, the Y[•] in β_2 oxidizes the cysteine residue in α_2 to the C[•] by a long-distance, intersubunit, proton-coupled electron-transfer (PCET) reaction (12) (vide infra).

Class I RNRs have been further subclassified as Ia–Ic. The Ia (e.g., from mammals) and Ib (e.g., from *Salmonella typhimurium*) enzymes both use the Fe^{III/III}-Y[•] cofactor but differ from each other in primary structure, allosteric regulatory behavior, and preference for the protein source of electrons for nucleotide reduction (3). These differences are functionally less profound than their shared difference from the Ic RNR(s). This third and most recently recognized subclass, of which the enzyme from the human pathogen *Chlamydia trachomatis* (Ct) is the founding member, is defined by the replacement of the radical-harboring Y in the β_2 subunit with the redox incompetent F (15, 16). We recently solved the seven-year mystery of how a class I RNR can be active without the initiating Y[•] by demonstrating that Ct RNR employs a stable, heterobinuclear, Mn^{IV}/Fe^{III} cofactor to initiate catalysis (17). Although the novel cofactor and radical-initiation strategy were just discovered, extensive analogy to the more extensively characterized class Ia *Ec* enzyme has served to focus initial studies, so that considerable insight has rapidly emerged and detailed working hypotheses can already be advanced. For proper context, we must briefly summarize what is known about the formation and function of the *Ec* RNR Fe₂^{III/III}-Y[•] cofactor before reviewing these studies on the novel Ct enzyme.

ACTIVATION OF *Ec* β_2

In assembly of the Fe₂^{III/III}-Y[•] cofactor, the Fe₂^{II/II} cluster reacts with O₂ to oxidize the buried tyrosine residue (Y122) by one electron (18, 19). The O₂-reactive complex forms spontaneously in vitro upon addition of Fe^{II} to apo β_2 , but it is possible that accessory factors (e.g., an iron chaperone) are involved in vivo. The reduced protein can also form by in situ reduction of the Fe₂^{III/III} cluster in the “met” protein (lacking the Y[•]). Indeed, reactivation of β_2 that has lost its Y[•] occurs by this mechanism in vivo and has been termed the “maintenance pathway” (20). The Fe₂S₂-containing ferredoxin, YfaE, and the flavodoxin, NrdI, have been identified as proteins that effect the Fe₂^{III/III} → Fe₂^{II/II} conversion for the class Ia and Ib β_2 s, respectively (21–23).

The mechanism of activation of wild-type (wt) *Ec* β_2 was investigated by a combination of rapid kinetic and spectroscopic methods (Figure 1, top) (12). An intermediate, termed X, was shown to be kinetically competent to oxidize Y122 in the last, slowest step of the reaction carried out in the presence of a reductant (e.g., ascorbate) (19, 24). X has an

$S = 1/2$ ground state that gives rise to a sharp, nearly isotropic $g = 2.0$ signal in the X-band EPR spectrum. Mössbauer and ⁵⁷Fe ENDOR spectroscopies revealed that the $S = 1/2$ ground state is a consequence of antiferromagnetic coupling between high-spin Fe^{III} ($S = 5/2$) and Fe^{IV} ($S = 2$) sites (25). X has been subjected to extensive spectroscopic (X-ray absorption, ¹H, ²H, and ¹⁷O ENDOR, and MCD) and computational analysis (25–29).

The complete reduction of O₂ at the Fe₂ cluster requires four electrons, of which three are provided by the oxidation of the reduced Fe₂^{II/II} cofactor to generate the Fe₂^{III/IV} intermediate, X. The transfer of the fourth (“extra”) electron to the diiron site is mediated by the near-surface residue, W48, which is transiently oxidized to a tryptophan cation radical (W48^{•+}) (30, 31). In vitro, the W48^{•+} is subsequently reduced by an exogenous reductant (e.g., ascorbate, a thiol, or Fe^{II}_{aq}) (31). The in vivo reductant for the W48^{•+} remains unclear, but the ferredoxin YfaE is a candidate (21).

Intermediates occurring before the X–W48^{•+} state barely accumulate during activation of wt *Ec* β_2 (31, 32) but have been observed in variants of the *Ec* protein and in the wt β_2 from mouse [*Mus musculus* (Mm)]. A (μ -1,2-peroxo)-Fe₂^{III/III} intermediate, which exhibits spectroscopic properties similar to those of the (μ -1,2-peroxo)-Fe₂^{III/III} intermediate, H_{peroxo} (or P), in the reaction of soluble methane monooxygenase (33), was observed in *Ec* β_2 variants with the D84E ligand substitution (34, 35) and, more importantly, in wt Mm β_2 (36). Insight into the immediate precursor to the X–W48^{•+} state was provided by studies on the *Ec* β_2 W48A/Y122F variant. 3-Methylindole was used as an analogue of the truncated W48 side chain to chemically trigger the ET step needed to form X (37). This precursor state comprises at least two distinct antiferromagnetically coupled Fe₂^{III/III} clusters, which may be protonated successors to the (μ -1,2-peroxo)-Fe₂^{III/III} intermediate.

PCET BETWEEN α_2 AND β_2

The distance in the *Ec* RNR holoenzyme between the Y[•] in β_2 and the C[•]-forming cysteine (C439) in α_2 is unknown but is ~35 Å in a “docking” model generated from the structures of the individual subunits (8). This model has been validated by pulsed electron–electron double resonance (PELDOR) and double-quantum coherence (DQC) measurements (38, 39). The rate constant for ET by a single electron-tunneling step over this long distance would be 10^{−4}–10^{−9} s^{−1}, which is far too slow to account for the single-turnover and steady-state rate constant of ~10 s^{−1} (25 °C) for *Ec* RNR (12). Rather, the ET is mediated by a chain of conserved, hydrogen-bonded, aromatic amino acids, including W48 and Y356 in *Ec* β_2 and Y731 and Y730 in *Ec* α_2 (Figure 2C), which form transient radicals in an “electron relay” mechanism (12). These residues are conserved in all known class I RNRs, and substitution of any of them with F leads to drastic diminution of activity (40–43). Further, the ET step is believed to be coupled to proton transfer [proton-coupled electron transfer (PCET)]. In the absence of environmental effects, pure ET (not proton-coupled) from a neutral C to a neutral Y[•] to give a Y^{•−}/C^{•+} state should be unfavorable. However, PCET to give a state with neutral constituents (Y/C[•]) is expected to be thermodynamically feasible (12). Thus, it is thought that the cysteine loses its proton and the tyrosine gains a proton in the PCET step.

² Some class I RNRs, e.g., the enzyme from *Homo sapiens*, can also have an $\alpha_4\beta_4$ and $\alpha_6\beta_6$ composition under certain conditions (14).

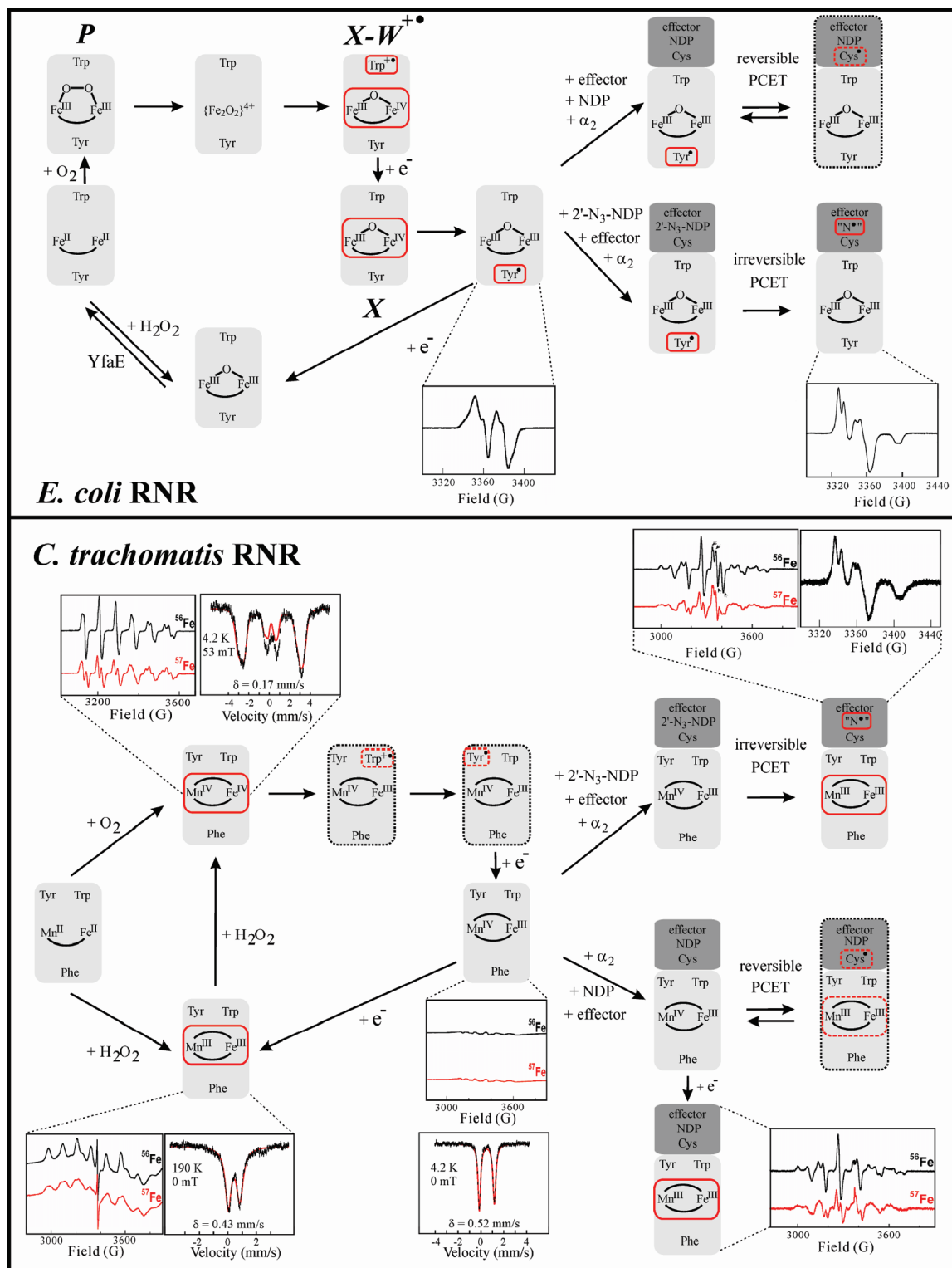


FIGURE 1: Assembly, maintenance, and role in catalysis of the Fe^{III}/III-Y* and Mn^{IV}/Fe^{III} cofactors of *Ec* β_2 (top) and *Ct* β_2 (bottom). The red boxes indicate EPR active states. States encircled with a gray dotted line have not been directly detected. Selected EPR and Mössbauer spectra of various states are also shown. The 3'-H-cleaving C* in α_2 has not been detected in either enzyme. However, copious indirect evidence, including structural analogy to the class II enzyme (12) in which the C* was directly detected (7), indicates that it forms in the *Ec* enzyme and by analogy the *Ct* enzyme. The spectrum of the N* in *Ec* RNR was adapted from ref 4.

Two obstacles long thwarted the direct interrogation of the PCET step. First, the forward PCET to generate the C* is preceded by a slow physical step, which is gated by the binding of a substrate and allosteric effector (PCET is thus said to be “conformationally gated”) (10). Consequently, intermediates are “kinetically masked”. Second,

although it is possible that the proposed pathway radical intermediates might still accumulate to low levels, their spectroscopic properties (in particular EPR) are expected to be similar to those of the Y122*, potentially preventing their detection. For these reasons, the studies of *Ec* β_2 activation stood for some time as the best evidence of a

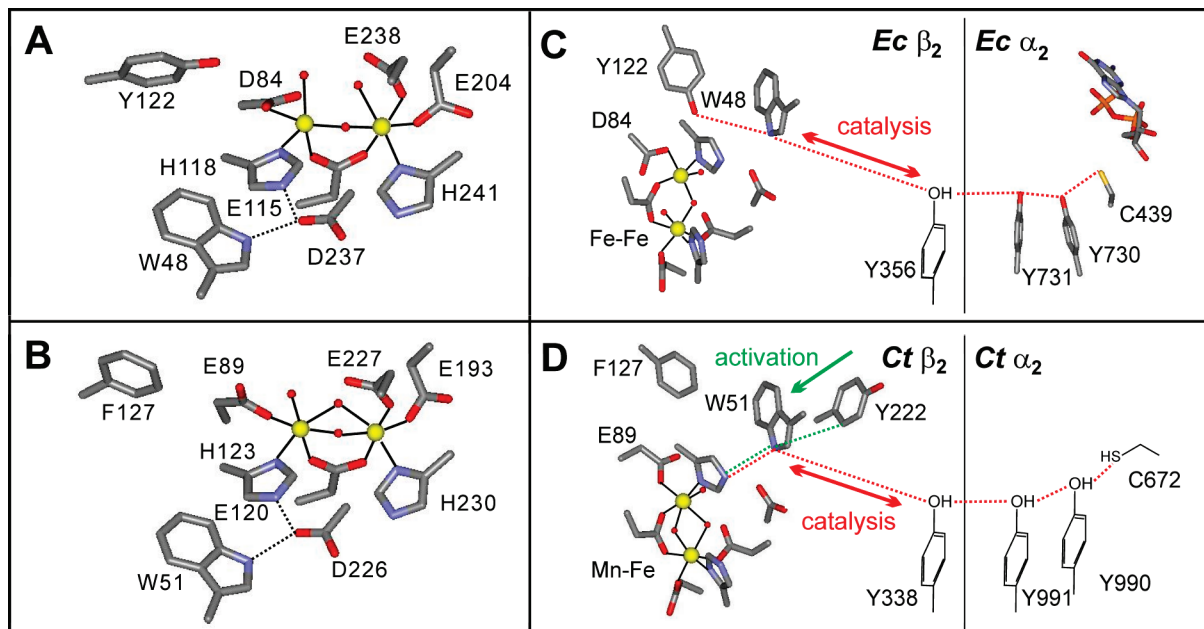


FIGURE 2: Structural models of the $\text{Fe}_2^{\text{III/III}}$ clusters in (A) *Ec* and (B) *Ct* β_2 s (Protein Data Bank entries 1MXR and 1SYY, respectively). Schematic representations of the proposed PCET pathways in (C) *Ec* and (D) *Ct* RNR. Panels C and D are adapted from refs 12 and 65, respectively.

radical-hopping mechanism for ET to the cofactor. In addition to establishing the role of W48 in relaying the “extra” electron, they also showed that W48^{++} can (under the proper conditions) oxidize Y122 (30, 31), which would be analogous to the last step in the reverse intersubunit PCET from Y122 to the C^* , and that a rapid redox equilibrium between W48 and Y356 is engaged in the presence of Mg^{2+} at concentrations similar to that employed in the RNR activity assay (15 mM) (44).

Stubbe and co-workers have at last provided definitive evidence for the proposed electron-relay PCET mechanism. First, by replacing the subunit-interfacial pathway tyrosine in the β_2 subunit of the *Ec* enzyme (Y356) with mono- and polyfluorinated tyrosines, they systematically varied the radical-reduction potential and pK_a of this pathway position. The catalytic activities (and their dependence on pH) of these variants established both the narrow range of reduction potential required for functional PCET and the fact that the Y356 phenolic proton is not obligatorily transferred (45). Second, by replacing any of the three pathway tyrosines (Y356 in β_2 or Y730 and Y731 in α_2) with a more easily oxidized analogue, they engineered depressions in the free-energy profile for the radical-hopping process, causing the radical to reside on the unnatural residue upon engagement of the ready holoenzyme complex (45–48). Importantly, the Y730/Y731 \rightarrow 3-aminotyrosine (NH_2Y) α_2 s retain significant catalytic activity, and the NH_2Y radicals detected in these variants are kinetically competent to be on the catalytic pathway (48).

DISCOVERY OF THE Y'-LESS CLASS I (Ic) RNR(S)

McClarty and co-workers isolated and sequenced the genes encoding the subunits of a class I RNR from the pathogenic intracellular parasite *C. trachomatis* (*Ct*) (15). Comparison of the predicted protein sequences to those of other RNR subunits revealed conservation of all but one of the β_2

cofactor ligands and all but one of the α_2 and β_2 PCET pathway residues (Figure 2). The important exceptions are the replacements of the radical-harboring Y with a redox-inert phenylalanine (F127) and the Fe1 aspartate ligand (D84 in *Ec* β_2) with glutamate (E89 in *Ct* β_2). The crystal structure of *Ct* β_2 confirmed that F127 is located at the site where the radical-harboring tyrosine is normally found (16). Despite the absence of the radical-harboring Y, the *Ct* RNR produced in and isolated from *Ec* was found to be catalytically active, suggesting a fundamentally different strategy for generating the C^* in the α_2 subunit (15). The $\text{Y} \rightarrow \text{F}$ and $\text{D} \rightarrow \text{E}$ nonidentities are also found in (hypothetical) β_2 proteins from other organisms, including the human pathogens *Mycobacterium tuberculosis* and *Tropheryma whipplei* (16). A third subclass, Ic, was created to comprise these Y'-less RNRs.

Nordlund, Gräslund, McClarty, and co-workers proposed that the $\text{Fe}_2^{\text{III/IV}}$ cluster, X, which they detected in the *Ct* β_2 protein by EPR spectroscopy, functionally replaces the Y^* of the conventional class I RNRs (16, 49). In support of this hypothesis, the stability of X was shown to be enhanced by the presence of α_2 (49). We recently confirmed an essential aspect of this innovative hypothesis: *Ct* RNR does indeed use a high-valent metal ion in place of the conventional Y^* as the radical initiator. However, the $\text{Fe}_2^{\text{III/IV}}$ complex of β_2 is not its active form. Rather, *Ct* RNR employs a $\text{Mn}^{\text{IV}}/\text{Fe}^{\text{III}}$ cofactor (50) to initiate catalysis (17).

DISCOVERY OF THE Mn REQUIREMENT OF CLASS Ic RNRs

We began our study of *Ct* RNR by measuring the catalytic activities of preparations of β_2 that had been isolated from different media and subjected to different metal-chelation and reconstitution procedures (17). We expected on the basis of the published hypothesis and previous studies on the *Ec* enzyme (51) to find a tight correlation between activity and iron content (Figure 3A). *Ct* β_2 emerged from the overproducing *Ec* cells grown in rich medium with 0.75 Fe/ β and a

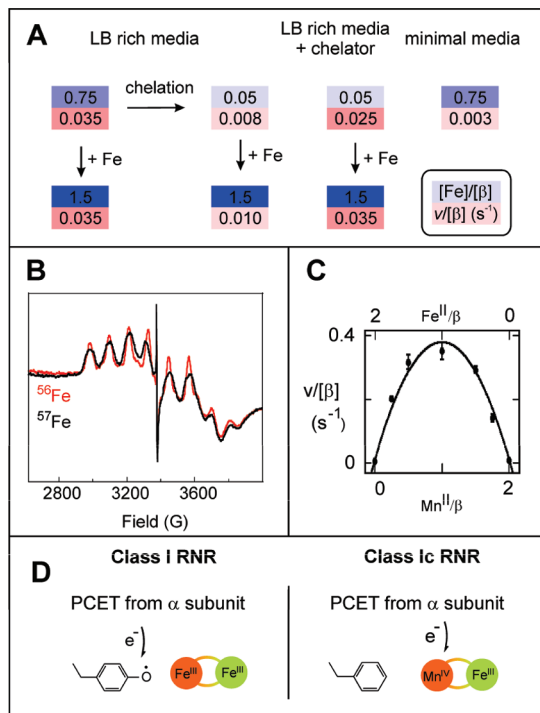


FIGURE 3: (A) Comparison of Fe per β (top, on the blue-shaded part) and activity per β (s^{-1}) (bottom, on the red-shaded part) for $Ct \beta_2$ prepared and treated in different ways. (B) EPR spectra of $Ct \beta_2$ that was isolated from *Ec* cells grown on rich medium, depleted of its Fe, reconstituted with 1.5 Fe^{II}/β (either natural abundance or $>95\%$ enriched ^{57}Fe), dialyzed to remove excess Fe, and reduced with 20 mM dithionite for 2 min at 22 °C. Spectrometer conditions: $T = 4$ K, $\nu = 9.45$ GHz, power = 20 mW, modulation amplitude = 10 G, scan time = 167 s, and time constant = 167 ms. (C) Dependence of the catalytic activity of $Ct \beta$ on the equivalencies of Mn^{II} and Fe^{II} at a constant total metal equivalency of $2/\beta$ (adapted from ref 17). (D) Schematic representation of the radical-generating cofactors of class Ia/b (left) and class Ic (right) RNRs (adapted from ref 50).

turnover number of $0.035 s^{-1}/\beta$, which is lower than the value reported by the Gräslund group [$0.05 s^{-1}$ (49)], and $<1\%$ of the optimal activity of the *Ec* protein (12). Addition of Fe^{II} in the presence of O_2 to reconstitute these preparations to full cofactor content (theoretically $2 Fe/\beta$) failed to increase activity. A reductive chelation procedure removed almost all the iron (leaving $<0.05/\beta$) and, as expected, diminished activity (to $\leq 0.008 s^{-1}$), but subsequent reconstitution of these preparations with excess Fe^{II} and O_2 increased activity only marginally, if at all (to $\leq 0.010 s^{-1}$). $Ct \beta_2$ purified from cells grown in the presence of the Fe^{II} chelator, 1,10-phenanthroline, had very little iron ($<0.05/\beta$) but greater than expected activity ($0.025 s^{-1}$). Addition of excess Fe^{II} to this protein in the presence of excess O_2 increased its activity only slightly (to $\leq 0.035 s^{-1}$). Finally, preparations from cells grown on minimal medium supplemented with iron had the same Fe content ($\sim 0.75 Fe/\beta$) as protein from rich medium but less than one-tenth of its activity ($\sim 0.003 s^{-1}$). The absence of the expected correlation between iron content and enzyme activity suggested the possibility of an additional cofactor component (17).

In parallel, we examined the $Ct \beta_2$ preparations subjected to the conditions described above and other treatments by a combination of spectroscopic methods. A multiline, $g \sim 2$ EPR spectrum (Figure 3B) exhibited by preparations reconstituted with Fe^{II} and then briefly treated with an excess of

the strong reductant, dithionite (17), was the crucial clue. Use of $^{57}Fe^{II}$ (with a nuclear spin quantum number, I , of $1/2$) in this treatment led to the broadening of several lines, indicating that the associated complex contains Fe. The multiple lines suggested hyperfine coupling to an additional transition metal with a high value of I , e.g., ^{55}Mn with an I of $5/2$. Aware of an earlier report of a similar EPR spectrum from a Mn^{III}/Fe^{III} complex (52), we considered that the dithionite-reduced $Ct \beta_2$ might harbor such a cluster. Following this spectroscopic clue, we examined the dependence of catalytic activity on the Mn/Fe ratio. Two equivalents of total metal ions was added to the metal-depleted protein with varying mole fractions of Mn and Fe, and the activity was monitored in the presence of O_2 (Figure 3C) (17). Addition of either Fe^{II} or Mn^{II} alone resulted in no significant increase over the residual activity (0.005 – $0.008 s^{-1}/\beta$) of the metal-depleted protein (a key point discussed further below), whereas addition of 1 equiv of each M^{II} activated the protein by a factor of more than 50 (17). These results strongly suggested that $Ct \beta_2$ uses a Mn/Fe cofactor rather than a Fe_2 cofactor.

A Mn^{IV}/Fe^{III} PRODUCT FROM REACTION OF THE Mn^{II}/Fe^{II} - β_2 COMPLEX WITH O_2

Reasoning by analogy to the conventional class I RNRs that the function of the $Ct \beta_2$ cofactor should be to oxidize the conserved cysteine in $Ct \alpha_2$ (C672) to the C^* , we anticipated that the reduced Mn^{II}/Fe^{II} - β_2 complex would be inactive and would be activated by reaction with O_2 . We verified this expectation by showing that addition of the O_2 -free Mn^{II}/Fe^{II} - β_2 complex to an RNR reaction solution also lacking O_2 did not result in turnover, whereas prior exposure of the complex to O_2 gave maximal activity, irrespective of the presence of O_2 in the subsequent RNR reaction (17). The stable (half-life of at least hours at 5 °C) product of the O_2 reaction is, by contrast to the active, Y^* -containing forms of the conventional β_2 proteins, EPR-silent.³ It exhibits a quadrupole doublet in the 4.2-K/zero-field Mössbauer spectrum (Figure 1). The isomer shift, $\delta = 0.52$ mm/s, indicates the presence of a high-spin Fe^{III} site. Its Mössbauer spectra in varying magnetic field show that it has an $S_{total} = 1$ ground state, which could most simply arise from antiferromagnetic coupling of the $S_{Fe} = 5/2$ Fe^{III} ion with an $S_{Mn} = 3/2$ Mn^{IV} site (50). The demonstration that the aforementioned dithionite treatment that gives the ^{55}Mn - and ^{57}Fe -coupled $g \sim 2$ EPR signal does not change the oxidation state of the Fe^{III} site confirmed this assignment by establishing that the $S_{total} = 1/2$ ground state of the dithionite-treated form arises from antiferromagnetic coupling of $S_{Fe} = 5/2$ Fe^{III} and $S_{Mn} = 2$ Mn^{III} ions (17). Thus, the product of the O_2 reaction in $Ct \beta_2$ (before its reduction by dithionite) is a Mn^{IV}/Fe^{III} complex. Like the product of the cognate reaction in a conventional β_2 , it is more oxidized than the $M_2^{II/III}$ reactant by three electrons (Figure 1).

THE Mn^{IV} SITE FUNCTIONALLY REPLACES THE Y^* OF A CONVENTIONAL CLASS I RNR

The next question was whether this stable product is the active form of $Ct \beta_2$. The inactivity of the dithionite-reduced

³ The absence of an EPR signal from the active form was at least partly responsible for the ~ 7 year interval between the discovery of the Y^* -less $Ct \beta_2$ and the correct identification of its functional cofactor.

Mn^{III}/Fe^{III} form was consistent with this possibility. The substrate analogue 2'-azido-2'-deoxyadenosine 5'-diphosphate (N₃-ADP) was used to confirm that the Mn^{IV}/Fe^{III} complex is the active form (17). In previous studies on *Ec* RNR, it had been shown that treatment with the 2'-azido-substituted nucleotide causes irreversible reduction of the Y[•] (53) along with formation of a meta-stable, nitrogen-centered radical (N[•]) (54) in which a cysteine of the enzyme is covalently linked to C3' via its sulfur and an N₃-derived nitrogen (55). Our expectation was that N₃-ADP would cause irreversible one-electron reduction of the *Ct* RNR radical initiator, resulting in conversion of the EPR-silent Mn^{IV}/Fe^{III} state to the EPR-active Mn^{III}/Fe^{III} state, together with formation of the N[•]. The spectrum of the N[•] was indeed observed. In addition, a spectrum with hyperfine coupling to both ⁵⁵Mn and ⁵⁷Fe was seen to develop in the N₃-ADP reaction but not in the reaction with the normal substrate, CDP. Although much sharper and more featured than the spectrum produced by dithionite treatment of β_2 in isolation, this spectrum was also seen upon dithionite treatment of the holoenzyme under turnover conditions.⁴ Parameters (**g**, **A**_{Mn}, and **A**_{Fe}) extracted by simulation of the spectrum, as well as more recent (unpublished) variable-field Mössbauer spectroscopic characterization of the N₃-ADP-generated species, establish that its cluster is in the Mn^{III}/Fe^{III} oxidation state. The reduction of the cluster by one electron concomitant with accumulation of the N[•] establishes that the EPR-silent, Mn^{IV}/Fe^{III} cluster is the radical initiator in *Ct* RNR. The observations also indicate that the EPR spectrum, and thus the structure, of the Mn^{III}/Fe^{III} cluster are sensitive to whether it is generated in isolated β_2 or the functioning holoenzyme. Presumably, binding of β_2 to $\alpha_2(\bullet\text{CDP}\cdot\text{ATP})$ causes a conformational change that is communicated to the cluster site. This change is likely to reflect the conformational gate for the PCET step (57).

After we had reported the activity of the Mn^{IV}/Fe^{III} form of *Ct* β_2 , the Gräslund group published a study also recognizing this fact (56). However, they interpreted their data to indicate that the Fe₂^{III/IV} form is also active (albeit less so). Our data are inconsistent with this view (17). Addition of Fe^{II} alone (in the presence of O₂) to metal-depleted (<0.05 Fe/ β) β_2 results in no significant increase in its RNR activity (<50% increase), even though the protein takes up the added Fe^{II} and the Fe₂^{III/IV} state, **X**, accumulates. By contrast, the optimized (Mn^{II} + Fe^{II}) reconstitution procedure activates the sample by ~100-fold (10000%). Moreover, treatment of the holoenzyme containing **X** in β_2 with N₃-ADP does not accelerate the very slow decay of **X** or cause accumulation of the N[•]. We view these observations as compelling evidence that the Fe₂^{III/IV} β_2 is inactive (17).

A Mn^{IV}/Fe^{IV} INTERMEDIATE DURING ACTIVATION OF *Ct* β_2

Further analysis of the activation reaction revealed accumulation of a novel Mn^{IV}/Fe^{IV} intermediate followed by the one-electron reduction of the Fe^{IV} site to give the active form (58). The Mn^{IV}/Fe^{IV} intermediate exhibits a broad

absorption feature centered near 390 nm and a sharp $g \sim 2$ EPR signal with six lines (from hyperfine coupling to a single ⁵⁵Mn nucleus) separated by ~80 G. When the intermediate contains ⁵⁷Fe, the sextet signal also shows hyperfine coupling to this $I = 1/2$ nucleus (Figure 1). The **A**_{Mn} tensor extracted from EPR simulation analysis is nearly isotropic (247, 216, 243 MHz), similar to **A**_{Mn} for the Mn^{IV} site in catalase (59). The Mössbauer isomer shift of the iron site ($\delta = 0.17 \pm 0.06$ mm/s) is indicative of the +IV oxidation state and is similar to that observed for the Fe₂^{IV/IV} complex, **Q**, in the reaction of sMMOH (33, 60). Field-dependent Mössbauer spectra show that the Fe^{IV} site is in the high spin ($S_{\text{Fe}} = 2$) configuration. Antiferromagnetic coupling between the Fe^{IV} ($S_{\text{Fe}} = 2$) and Mn^{IV} ($S_{\text{Mn}} = 3/2$) ions results in the $S = 1/2$ ground state (58). To the best of our knowledge, the Mn^{IV}/Fe^{IV} complex has no precedent in either inorganic chemistry or biochemistry. It is the cognate of the Fe₂^{IV/IV} intermediate **Q** from sMMO (33, 60, 61). It is likely to have a di- μ -oxo-Mn^{IV}/Fe^{IV} "diamond core" structure, which was suggested for **Q** (62). The crystal structure of the Fe₂^{III/III} form of β_2 revealed the presence of two solvent (water or hydroxo) bridges (16) (Figure 2A), which contrasts with the single oxo bridge found in the class Ia (63) (Figure 2B) and Ib β_2 s (64). This difference suggests that the *Ct* β_2 site could be adapted to stabilize the diamond core in the Mn^{IV}/Fe^{IV} and Mn^{IV}/Fe^{III} states. Formation of the Mn^{IV}/Fe^{IV} intermediate is first-order in O₂ concentration ($k_{\text{form}} = 13 \pm 3 \text{ mM}^{-1} \text{ s}^{-1}$ at 5 °C) (58). Thus, intermediates preceding the Mn^{IV}/Fe^{IV} state [e.g., a peroxo-Mn^{III}/Fe^{III} analogue of the μ -1,2-peroxo-Fe₂^{III/III} complex detected during activation of the *Mm* (36) and *Ec* (32) proteins] do not accumulate. The EPR-active, $S = 1/2$ ground state of the Mn^{IV}/Fe^{IV} intermediate makes it amenable to structural characterization by multinuclear paramagnetic resonance methods (27), an opportunity not afforded by the homobinuclear homologue, **Q**, with its diamagnetic ground state.⁵

EVIDENCE FOR BRANCHED ELECTRON-RELAY PATHWAYS IN *Ct* β_2

The Mn^{IV}/Fe^{IV} state decays to the stable Mn^{IV}/Fe^{III} state by transfer of the extra electron to the Fe^{IV} site (58). The "intrinsic" decay rate constant is $0.02 \pm 0.005 \text{ s}^{-1}$ (5 °C), and the process is accelerated by the reductant, ascorbate, with a second-order rate constant of $1.3 \pm 0.3 \text{ mM}^{-1} \text{ s}^{-1}$ (58). In activation of *Ec* β_2 , the extra electron is relayed to the cluster by W48, which is transiently oxidized to the W48⁺⁺ (31). In *Ct* β_2 , the surface residue Y222 plays a key role in the electron relay (65). The rate constants for intrinsic decay and ascorbate reduction are diminished by 10- and 65-fold, respectively, in the Y222F variant. The same product (the Mn^{IV}/Fe^{III} cluster) still forms, and the Y222F protein is then as active as the wild-type protein, establishing that Y222 is not part of the intersubunit PCET pathway (Figure 2D). Conversely, substitution of Y338, the counterpart of the

⁴ After we reported the spectrum of the Mn^{III}/Fe^{III} cluster generated by treatment of the holoenzyme with either dithionite or N₃-ADP, Gräslund and co-workers reported that treatment with hydroxyurea can generate the same spectrum (56).

⁵ Conversion of the diamagnetic Fe₂^{IV/IV} intermediate **Q** to the paramagnetic Fe₂^{III/IV} form with an $S = 1/2$ ground state by γ -radiolytic cryoreduction has been reported (70). However, the EPR signal of the resulting cluster overlaps with the signals from the organic radicals produced by this procedure and does not permit the detailed ENDOR-spectroscopic characterization of the Fe₂^{III/IV} state, as was reported for the Fe₂^{III/IV} intermediate **X** from *Ec* β_2 (25, 27).

subunit-interfacial PCET-pathway residue (Y356) in *Ec* β_2 (40, 47), with F does not affect the kinetics of the activation reaction but diminishes the catalytic activity to an undetectable level. Substitution of W51, the counterpart of *Ec* β_2 W48, with F compromises both activation and catalysis, marking this residue as the branch point for the activation- and catalysis-specific pathways (65).

REACTION OF THE $\text{Mn}^{\text{III}}/\text{Fe}^{\text{III}}$ AND $\text{Mn}^{\text{II}}/\text{Fe}^{\text{II}}$ FORMS WITH H_2O_2

Before our identification of its unique cofactor, it had been suggested that the Y⁻-less class Ic β_2 s might have evolved to tolerate oxidative stress imposed by the host's immune response (16). Our examination of the reactivities of the $\text{Mn}^{\text{IV}}/\text{Fe}^{\text{III}}$, $\text{Mn}^{\text{III}}/\text{Fe}^{\text{III}}$, and $\text{Mn}^{\text{II}}/\text{Fe}^{\text{II}}$ forms of *Ct* β_2 toward hydrogen peroxide, an important host-generated reactive oxygen species (ROS), is consistent with this notion (66). The $\text{Mn}^{\text{IV}}/\text{Fe}^{\text{III}}$ form is completely stable in the presence of H_2O_2 and retains full activity. The inactive, one-electron-reduced $\text{Mn}^{\text{III}}/\text{Fe}^{\text{III}}$ form is rapidly ($8 \pm 1 \text{ M}^{-1} \text{ s}^{-1}$ at 5 °C) and quantitatively (>90%) reactivated by H_2O_2 via the $\text{Mn}^{\text{IV}}/\text{Fe}^{\text{IV}}$ intermediate. The fully reduced $\text{Mn}^{\text{II}}/\text{Fe}^{\text{II}}$ form is also efficiently activated in a three-step reaction through $\text{Mn}^{\text{III}}/\text{Fe}^{\text{III}}$ and $\text{Mn}^{\text{IV}}/\text{Fe}^{\text{IV}}$ intermediates (see Figure 1). The propensity of *Ct* β_2 to become fully active upon exposure to H_2O_2 essentially irrespective of its initial redox state represents a potentially relevant contrast to the behavior of the *Ec* protein. Although its fully reduced ($\text{Fe}_2^{\text{II/III}}$) state reacts readily with H_2O_2 to generate the "met" (Y⁻-less) $\text{Fe}_2^{\text{III/III}}$ form, this form further reacts only very inefficiently to generate the active Y⁻-containing protein (67).

OUTLOOK

Our recent work has demonstrated that nature chose a decidedly bioinorganic solution to replacement of the radical-initiating Y⁻- $\text{Fe}_2^{\text{III/III}}$ cofactor of a conventional class I RNR: the use of a high-valent Mn^{IV} site in a $\text{Mn}^{\text{IV}}/\text{Fe}^{\text{III}}$ cluster. To our knowledge, *Ct* RNR provides the first example of a heterobinuclear Mn/Fe redox cofactor in biology and the only uncontradicted example of a Mn-containing RNR.⁶ Its use of the Mn/Fe cofactor affords unique opportunities to dissect the conformationally gated, intersubunit, long-distance PCET. The absence of an EPR signal from the resting *Ct* enzyme could permit detection of even trace levels of pathway radicals that in the conventional RNRs might be obscured by the spectrum of the initiating Y[•]. In addition, by contrast to the best-studied conventional class I RNR from *Ec*, the reduced form of the cofactor ($\text{Mn}^{\text{III}}/\text{Fe}^{\text{III}}$) in *Ct* RNR is EPR-active, and its structure is apparently sensitive to remote binding events. Efforts to capitalize on these opportunities are underway.

ACKNOWLEDGMENT

We thank our colleagues whose work is reviewed herein.

⁶ It was initially reported that the class I RNR from *Corynebacterium ammoniagenes* (formerly called *Brevibacterium ammoniagenes*) uses a Mn-containing cofactor of unknown composition (68). Recent studies suggest that this RNR can utilize the conventional Y⁻- $\text{Fe}_2^{\text{III/III}}$ cofactor (69). This controversy is one of several, recent, stark illustrations of the importance of correlating catalytic activity with metal (cluster) content of a redox metalloenzyme in identifying its functional cofactor.

REFERENCES

- Licht, S., and Stubbe, J. (1999) Mechanistic investigations of ribonucleotide reductases. In *Comprehensive natural products chemistry* (Poulter, C. D., Ed.) pp 163–203, Elsevier, New York.
- Nordlund, P., and Reichard, P. (2006) Ribonucleotide reductases. *Annu. Rev. Biochem.* 75, 681–706.
- Reichard, P. (1997) The evolution of ribonucleotide reduction. *Trends Biochem. Sci.* 22, 81–85.
- Stubbe, J., and van der Donk, W. A. (1998) Protein radicals in enzyme catalysis. *Chem. Rev.* 98, 705–762.
- Mao, S. S., Yu, G. X., Chalfoun, D., and Stubbe, J. (1992) Characterization of C439SR1, a mutant of *Escherichia coli* ribonucleotide diphosphate reductase: Evidence that C439 is a residue essential for nucleotide reduction and C439SR1 is a protein possessing novel thioredoxin-like activity. *Biochemistry* 31, 9752–9759.
- Mao, S. S., Holler, T. P., Yu, G. X., Bollinger, J. M., Jr., Booker, S., Johnston, M. I., and Stubbe, J. (1992) A model for the role of multiple cysteine residues involved in ribonucleotide reduction: Amazing and still confusing. *Biochemistry* 31, 9733–9743.
- Licht, S., Gerfen, G. J., and Stubbe, J. (1996) Thyl radicals in ribonucleotide reductases. *Science* 271, 477–481.
- Uhlen, U., and Eklund, H. (1994) Structure of ribonucleotide reductase protein R1. *Nature* 370, 533–539.
- Stubbe, J., and Ackles, D. (1980) On the mechanism of ribonucleoside diphosphate reductase from *Escherichia coli*. *J. Biol. Chem.* 255, 8027–8030.
- Ge, J., Yu, G., Ator, M. A., and Stubbe, J. (2003) Pre-steady-state and steady-state kinetic analysis of *E. coli* class I ribonucleotide reductase. *Biochemistry* 42, 10017–10083.
- Licht, S. S., Lawrence, C. C., and Stubbe, J. (1999) Class II ribonucleotide reductases catalyze carbon-cobalt bond reformation on every turnover. *J. Am. Chem. Soc.* 121, 7463–7468.
- Stubbe, J., Nocera, D. G., Yee, C. S., and Chang, M. C. Y. (2003) Radical initiation in the class I ribonucleotide reductase: Long-range proton-coupled electron transfer? *Chem. Rev.* 103, 2167–2202.
- Stubbe, J. (2003) Di-iron-tyrosyl radical ribonucleotide reductases. *Curr. Opin. Chem. Biol.* 7, 183–188.
- Kashlan, O. B., Scott, C. P., Lear, J. D., and Cooperman, B. S. (2002) A comprehensive model for the allosteric regulation of mammalian ribonucleotide reductase. Functional consequences of ATP- and dATP-induced oligomerization of the large subunit. *Biochemistry* 41, 462–474.
- Roshick, C., Iliffe-Lee, E. R., and McClarty, G. (2000) Cloning and characterization of ribonucleotide reductase from *Chlamydia trachomatis*. *J. Biol. Chem.* 275, 38111–38119.
- Högbom, M., Stenmark, P., Voevodskaya, N., McClarty, G., Gräslund, A., and Nordlund, P. (2004) The radical site in Chlamydial ribonucleotide reductase defines a new R2 subclass. *Science* 305, 245–248.
- Jiang, W., Yun, D., Saleh, L., Barr, E. W., Xing, G., Hoffart, L. M., Maslak, M.-A., Krebs, C., and Bollinger, J. M., Jr. (2007) A manganese(IV)/iron(III) cofactor in *Chlamydia trachomatis* ribonucleotide reductase. *Science* 316, 1188–1191.
- Petersson, L., Gräslund, A., Ehrenberg, A., Sjöberg, B.-M., and Reichard, P. (1980) The iron center in ribonucleotide reductase from *Escherichia coli*. *J. Biol. Chem.* 255, 6706–6712.
- Bollinger, J. M., Jr., Edmondson, D. E., Huynh, B. H., Filley, J., Norton, J. R., and Stubbe, J. (1991) Mechanism of assembly of the tyrosyl radical-dinuclear iron cluster cofactor of ribonucleotide reductase. *Science* 253, 292–298.
- Hristova, D., Wu, C.-H., Jiang, W., Krebs, C., and Stubbe, J. (2008) Importance of the maintenance pathway in the regulation of the activity of *Escherichia coli* ribonucleotide reductase. *Biochemistry* 47, 3989–3999.
- Wu, C.-H., Jiang, W., Krebs, C., and Stubbe, J. (2007) YfaE, a ferredoxin involved in diferric-tyrosyl radical maintenance in *Escherichia coli* ribonucleotide reductase. *Biochemistry* 46, 11577–11588.
- Roca, I., Torrents, E., Sahlin, M., Gibert, I., and Sjöberg, B.-M. (2008) NrdI essentiality for class Ib ribonucleotide reduction in *Streptococcus pyogenes*. *J. Bacteriol.* 190, 4849–4858.
- Cotruvo, J. A., Jr., and Stubbe, J. (2008) NrdI, an unusual flavodoxin involved in maintenance of the diferric-tyrosyl radical cofactor in *Escherichia coli* class Ib ribonucleotide reductase. *Proc. Natl. Acad. Sci. U.S.A.* 105, 14383–14388.

24. Bollinger, J. M., Jr., Tong, W. H., Ravi, N., Huynh, B. H., Edmondson, D. E., and Stubbe, J. (1994) Mechanism of assembly of the tyrosyl radical-diiron(III) cofactor of *E. coli* ribonucleotide reductase. 2. Kinetics of the excess Fe^{2+} reaction by optical, EPR, and Mössbauer spectroscopies. *J. Am. Chem. Soc.* **116**, 8015–8023.
25. Sturgeon, B. E., Burdi, D., Chen, S., Huynh, B. H., Edmondson, D. E., Stubbe, J., and Hoffman, B. M. (1996) Reconsideration of **X**, the diiron intermediate formed during cofactor assembly in *E. coli* ribonucleotide reductase. *J. Am. Chem. Soc.* **118**, 7551–7557.
26. Riggs-Gelasco, P. J., Shu, L., Chen, S., Burdi, D., Huynh, B. H., Que, L., Jr., and Stubbe, J. (1998) EXAFS characterization of the intermediate **X** generated during the assembly of the *Escherichia coli* ribonucleotide reductase R2 diferric tyrosyl radical cofactor. *J. Am. Chem. Soc.* **120**, 849–860.
27. Burdi, D., Willems, J.-P., Riggs-Gelasco, P., Antholine, W. E., Stubbe, J., and Hoffman, B. M. (1998) The core structure of **X** generated in the assembly of the diiron cluster of ribonucleotide reductase: $^{17}\text{O}_2$ and H_2^{17}O ENDOR. *J. Am. Chem. Soc.* **120**, 12910–12919.
28. Mitić, N., Clay, M. D., Saleh, L., Bollinger, J. M., Jr., and Solomon, E. I. (2007) Spectroscopic and electronic structure studies of intermediate **X** in ribonucleotide reductase R2 and two variants: A description of the Fe^{IV} -oxo bond in the Fe^{III} -O- Fe^{IV} dimer. *J. Am. Chem. Soc.* **129**, 9049–9065.
29. Han, W.-G., Liu, T., Lovell, T., and Noodleman, L. (2006) Density functional theory study of $\text{Fe}(\text{IV})$ d-d optical transitions in active-site models of class I ribonucleotide reductase intermediate **X** with vertical self-consistent reaction field methods. *Inorg. Chem.* **45**, 8533–8542.
30. Bollinger, J. M., Jr., Tong, W. H., Ravi, N., Huynh, B. H., Edmondson, D. E., and Stubbe, J. (1994) Mechanism of assembly of the tyrosyl radical-diiron(III) cofactor of *E. coli* ribonucleotide reductase. 3. Kinetics of the limiting Fe^{2+} reaction by optical, EPR, and Mössbauer spectroscopies. *J. Am. Chem. Soc.* **116**, 8024–8032.
31. Baldwin, J., Krebs, C., Ley, B. A., Edmondson, D. E., Huynh, B. H., and Bollinger, J. M., Jr. (2000) Mechanism of rapid electron transfer during oxygen activation in the R2 subunit of *Escherichia coli* ribonucleotide reductase. 1. Evidence for a transient tryptophan radical. *J. Am. Chem. Soc.* **122**, 12195–12206.
32. Tong, W. H., Chen, S., Lloyd, S. G., Edmondson, D. E., Huynh, B. H., and Stubbe, J. (1996) Mechanism of assembly of the diferric cluster-tyrosyl radical cofactor of *Escherichia coli* ribonucleotide reductase from the diferrous form of the R2 subunit. *J. Am. Chem. Soc.* **118**, 2107–2108.
33. Liu, K. E., Valentine, A. M., Wang, D., Huynh, B. H., Edmondson, D. E., Salifoglou, A., and Lippard, S. J. (1995) Kinetic and spectroscopic characterization of intermediates and component interactions in reactions of methane monooxygenase from *Methylococcus capsulatus* (Bath). *J. Am. Chem. Soc.* **117**, 10174–10185.
34. Bollinger, J. M., Jr., Krebs, C., Vicol, A., Chen, S., Ley, B. A., Edmondson, D. E., and Huynh, B. H. (1998) Engineering the diiron site of *Escherichia coli* ribonucleotide reductase protein R2 to accumulate an intermediate similar to H_{peroxo} , the putative peroxo-diiron(III) complex from the methane monooxygenase catalytic cycle. *J. Am. Chem. Soc.* **120**, 1094–1095.
35. Skulan, A. J., Brunold, T. C., Baldwin, J., Saleh, L., Bollinger, J. M., Jr., and Solomon, E. I. (2004) Nature of the peroxo intermediate of the W48F/D84E ribonucleotide reductase variant: Implications for O_2 activation by binuclear non-heme iron enzymes. *J. Am. Chem. Soc.* **126**, 8842–8855.
36. Yun, D., García-Serres, R., Chicalese, B. M., An, Y. H., Huynh, B. H., and Bollinger, J. M., Jr. (2007) $(\mu\text{-}1,2\text{-Perox})\text{diiron(III/III)}$ complex as a precursor to the diiron(III/IV) intermediate **X** in the assembly of the iron-radical cofactor of ribonucleotide reductase from mouse. *Biochemistry* **46**, 1925–1932.
37. Saleh, L., Krebs, C., Ley, B. A., Naik, S., Huynh, B. H., and Bollinger, J. M., Jr. (2004) Use of a chemical trigger for electron transfer to characterize a precursor to cluster **X** in assembly of the iron-radical cofactor of *Escherichia coli* ribonucleotide reductase. *Biochemistry* **43**, 5953–5964.
38. Bennati, M., Weber, A., Antonic, J., Perlstein, D. L., Robblee, J. H., and Stubbe, J. (2003) Pulsed ELDOR spectroscopy measures the distance between the two tyrosyl radicals in the R2 subunit of the *E. coli* ribonucleotide reductase. *J. Am. Chem. Soc.* **125**, 14988–14989.
39. Bennati, M., Robblee, J. H., Mugnaini, V., Stubbe, J., Freed, J. H., and Borbat, P. (2005) EPR distance measurements support a model for long-range radical initiation in *E. coli* ribonucleotide reductase. *J. Am. Chem. Soc.* **127**, 15014–15015.
40. Climent, I., Sjöberg, B.-M., and Huang, C. Y. (1992) Site-directed mutagenesis and deletion of the carboxyl terminus of *Escherichia coli* ribonucleotide reductase protein R2. Effects on catalytic activity and subunit interaction. *Biochemistry* **31**, 4801–4807.
41. Ekberg, M., Sahlin, M., Eriksson, M., and Sjöberg, B.-M. (1996) Two conserved tyrosine residues in protein R1 participate in an intermolecular electron transfer in ribonucleotide reductase. *J. Biol. Chem.* **271**, 20655–20659.
42. Rova, U., Goodtzova, K., Ingemarson, R., Behravan, G., Gräslund, A., and Thelander, L. (1995) Evidence by site-directed mutagenesis supports long-range electron transfer in mouse ribonucleotide reductase. *Biochemistry* **34**, 4267–4275.
43. Rova, U., Adrait, A., Pötsch, S., Gräslund, A., and Thelander, L. (1999) Evidence by mutagenesis that Tyr^{370} of the mouse ribonucleotide reductase R2 protein is the connecting link in the intersubunit radical transfer pathway. *J. Biol. Chem.* **274**, 23746–23751.
44. Saleh, L., and Bollinger, J. M., Jr. (2006) Cation mediation of radical transfer between Trp48 and Tyr356 during O_2 activation by protein R2 of *Escherichia coli* ribonucleotide reductase: Relevance to R1-R2 radical transfer in nucleotide reduction. *Biochemistry* **45**, 8823–8830.
45. Seyedsayamdost, M. R., Yee, C. S., Reece, S. Y., Nocera, D. G., and Stubbe, J. (2006) pH rate profiles of $\text{F}_n\text{Y}_{356}\text{-R}_2\text{s}$ ($n = 2, 3, 4$) in *Escherichia coli* ribonucleotide reductase: Evidence that Y_{356} is a redox-active amino acid along the radical propagation pathway. *J. Am. Chem. Soc.* **128**, 1562–1568.
46. Seyedsayamdost, M. R., and Stubbe, J. (2006) Site-specific replacement of Y356 with 3,4-dihydroxyphenylalanine in the $\beta 2$ subunit of *E. coli* ribonucleotide reductase. *J. Am. Chem. Soc.* **128**, 2522–2523.
47. Seyedsayamdost, M. R., and Stubbe, J. (2007) Forward and reverse electron transfer with the $\text{Y}_{356}\text{DOPA-}\beta 2$ heterodimer of *E. coli* ribonucleotide reductase. *J. Am. Chem. Soc.* **129**, 2226–2227.
48. Seyedsayamdost, M. R., Xie, J., Chan, C. T. Y., Schultz, P. G., and Stubbe, J. (2007) Site-specific insertion of 3-aminotyrosine into subunit $\alpha 2$ of *E. coli* ribonucleotide reductase: Direct evidence for involvement of Y_{730} and Y_{731} in radical propagation. *J. Am. Chem. Soc.* **129**, 15060–15071.
49. Voevodskaya, N., Narvaez, A. J., Domkin, V., Torrents, E., Thelander, L., and Gräslund, A. (2006) Chlamydial ribonucleotide reductase: Tyrosyl radical function in catalysis replaced by the Fe^{III} - Fe^{IV} cluster. *Proc. Natl. Acad. Sci. U.S.A.* **103**, 9850–9854.
50. Jiang, W., Bollinger, J. M., Jr., and Krebs, C. (2007) The active form of *Chlamydia trachomatis* ribonucleotide reductase R2 protein contains a heterodinuclear Mn(IV)/Fe(III) cluster with $S = 1$ ground state. *J. Am. Chem. Soc.* **129**, 7504–7505.
51. Atkin, C. L., Thelander, L., Reichard, P., and Lang, G. (1973) Iron and free radical in ribonucleotide reductase. Exchange of iron and Mössbauer spectroscopy of the protein B2 subunit of the *Escherichia coli* enzyme. *J. Biol. Chem.* **248**, 7464–7472.
52. Bossek, U., Weyhermüller, T., Wieghardt, K., Bonvoisin, J., and Gierd, J. J. (1989) Synthesis, E.S.R. spectrum and magnetic properties of a heterodinuclear complex containing the $\{\text{Fe}^{\text{III}}(\mu\text{-O})(\mu\text{-MeCO}_2)_2\text{Mn}^{\text{III}}\}^{2+}$ core. *J. Chem. Soc., Chem. Commun.* **10**, 633–636.
53. Thelander, L., Larsson, B., Hobbs, J., and Eckstein, F. (1976) Active site of ribonucleoside diphosphate reductase from *Escherichia coli*. Inactivation of the enzyme by 2'-substituted ribonucleoside diphosphates. *J. Biol. Chem.* **251**, 1398–1405.
54. Sjöberg, B.-M., Gräslund, A., and Eckstein, F. (1983) A substrate radical intermediate in the reaction between ribonucleotide reductase from *Escherichia coli* and 2'-azido-2'-deoxyribonucleoside diphosphates. *J. Biol. Chem.* **258**, 8060–8067.
55. Fritscher, J., Artin, E., Wnuk, S., Bar, G., Robblee, J. H., Kacprzak, S., Kaupp, M., Griffin, R. G., Bennati, M., and Stubbe, J. (2005) Structure of the nitrogen-centered radical formed during inactivation of *E. coli* ribonucleotide reductase by 2'-azido-2'-deoxyuridine-5'-diphosphate: Trapping of the 3'-ketonucleotide. *J. Am. Chem. Soc.* **127**, 7729–7738.
56. Voevodskaya, N., Lendzian, F., Ehrenberg, A., and Gräslund, A. (2007) High catalytic activity achieved with a mixed manganese-iron site in protein R2 of *Chlamydia* ribonucleotide reductase. *FEBS Lett.* **581**, 3351–3355.
57. Bollinger, J. M., Jr., Jiang, W., Green, M. T., and Krebs, C. (2008) The manganese(IV)/iron(III) cofactor of *Chlamydia trachomatis* ribonucleotide reductase: Structure, assembly, radical initiation, and evolution. *Curr. Opin. Struct. Biol.*, DOI: 10.1016/j.sbi.2008.11.007.

58. Jiang, W., Hoffart, L. M., Krebs, C., and Bollinger, J. M., Jr. (2007) A manganese(IV)/iron(IV) intermediate in assembly of the manganese(IV)/iron(III) cofactor of *Chlamydia trachomatis* ribonucleotide reductase. *Biochemistry* 46, 8709–8716.
59. Zheng, M., Khangulov, S. V., Dismukes, G. C., and Barynin, V. V. (1994) Electronic structure of dimanganese(II,III) and dimanganese(III,IV) complexes and dimanganese catalase enzyme: A general EPR spectral simulation approach. *Inorg. Chem.* 33, 382–387.
60. Lee, S.-K., Fox, B. G., Froland, W. A., Lipscomb, J. D., and Münck, E. (1993) A transient intermediate of the methane monooxygenase catalytic cycle containing an $\text{Fe}^{\text{IV}}\text{Fe}^{\text{IV}}$ cluster. *J. Am. Chem. Soc.* 115, 6450–6451.
61. Lee, S. K., Nesheim, J. C., and Lipscomb, J. D. (1993) Transient intermediates of the methane monooxygenase catalytic cycle. *J. Biol. Chem.* 268, 21569–21577.
62. Shu, L., Nesheim, J. C., Kauffmann, K. E., Münck, E., Lipscomb, J. D., and Que, L., Jr. (1997) An $\text{Fe}_2^{\text{IV}}\text{O}_2$ diamond core structure for the key intermediate **Q** of methane monooxygenase. *Science* 275, 515–518.
63. Nordlund, P., Sjöberg, B.-M., and Eklund, H. (1990) Three-dimensional structure of the free radical protein of ribonucleotide reductase. *Nature* 345, 593–598.
64. Eriksson, M., Jordan, A., and Eklund, H. (1998) Structure of *Salmonella typhimurium* nrdF ribonucleotide reductase in its oxidized and reduced forms. *Biochemistry* 37, 13359–13369.
65. Jiang, W., Saleh, L., Barr, E. W., Xie, J., Maslak Gardner, M., Krebs, C., and Bollinger, J. M., Jr. (2008) Branched activation- and catalysis-specific pathways for electron relay to the manganese/iron cofactor in ribonucleotide reductase from *Chlamydia trachomatis*. *Biochemistry* 47, 8477–8484.
66. Jiang, W., Xie, J., Nørgaard, H., Bollinger, J. M., Jr., and Krebs, C. (2008) Rapid and quantitative activation of *Chlamydia trachomatis* ribonucleotide reductase by hydrogen peroxide. *Biochemistry* 47, 4477–4483.
67. Sahlin, M., Sjöberg, B.-M., Backes, G., Loehr, T., and Sanders-Loehr, J. (1990) Activation of the iron-containing B2 protein of ribonucleotide reductase by hydrogen peroxide. *Biochem. Biophys. Res. Commun.* 167, 813–818.
68. Willing, A., Follmann, H., and Auling, G. (1988) Ribonucleotide reductase of *Brevibacterium ammoniagenes* is a manganese enzyme. *Eur. J. Biochem.* 170, 603–611.
69. Huque, Y., Fieschi, F., Torrents, E., Gibert, I., Eliasson, R., Reichard, P., Sahlin, M., and Sjöberg, B.-M. (2000) The active form of the R2F protein of class Ib ribonucleotide reductase from *Corynebacterium ammoniagenes* is a diferric protein. *J. Biol. Chem.* 275, 25365–25371.
70. Valentine, A. M., Tavares, P., Pereira, A. S., Davydov, R., Krebs, C., Hoffman, B. M., Edmondson, D. E., Huynh, B. H., and Lippard, S. J. (1998) Characterization of a mixed-valent $\text{Fe}(\text{III})\text{Fe}(\text{IV})$ form of intermediate **Q** in the reaction cycle of soluble methane monooxygenase, an analog of intermediate **X** in ribonucleotide reductase R2 assembly. *J. Am. Chem. Soc.* 120, 2190–2191.

BI8017625